

## First-Principle Calculation-Assisted Structural Study on the Nanoscale Phase Transition of Si for Li-Ion Secondary Batteries

Yong-Mook Kang,<sup>\*†</sup> Seung-Bum Suh,<sup>‡</sup> and Yang-Soo Kim<sup>§</sup>

<sup>†</sup>Division of Advanced Materials Engineering, Kongju National University, 275 Budae-dong, Cheonan, Chungnam, Republic of Korea, <sup>‡</sup>Energy Lab, Samsung SDI Co., LTD, 428-5, Gongse-ri, Giheung-eup, Yongin-si, Gyeonggi-do, Republic of Korea, and <sup>§</sup>Sunchon Branch, Korea Basic Science Institute, 315 Maegok, Suncheon, Jeonranam-do, Republic of Korea

Received August 21, 2009

The CASTEP ab initio calculation was coupled with TEM-EELS analysis to elucidate the nanostructural change of Si during Li<sup>+</sup> insertion. Even if the previous research alleged that Si should change into amorphous lithium silicide in the initial stage of Li<sup>+</sup> insertion, our observation let us know that during the electrochemical Li<sup>+</sup> insertion, Si transforms into LiSi with medium-range ordering, and finally into a well-known crystalline phase, Li<sub>15</sub>Si<sub>4</sub>. Because some macroscopic observation (such as the volume expansion and charge–discharge behaviors) is almost in accordance with the microstructural analysis for this clarified phase transition, we can say that the correlation between experimental edge spectra and theoretical calculation based on density functional theory is very meaningful way to clarify the phase transition of materials.

### Introduction

With an advent of the ubiquitous era, the demand for rechargeable batteries with a higher energy density is getting more and more critical. It is because applications are emerging such as electric vehicles and various types of portable electronic devices. Carbonaceous materials are commonly adopted as the anode material for commercial lithium-ion secondary batteries because they can reversibly intercalate or deintercalate Li ions. However, the low capacity of carbon (theoretical capacity, 372 mA h g<sup>-1</sup>) has become a limiting factor in wider applications, and a high capacity alternative to carbonaceous material has thus been sought.<sup>1–3</sup> Even if silicon has been considered as one of the most attractive options for high energy density purposes, its poor cyclic properties have been delaying its commercialization.<sup>4</sup>

In previous research, the cyclic degradation of Si-based materials could be primarily attributed to two reasons: (i) huge volume expansion of Si, followed by a loss of electronic

contact; and (ii) inhomogeneous Li<sup>+</sup> insertion induced by low electronic conductivity of Si.<sup>5–7</sup> The difficulty of structural analyses, caused by a complete disappearance of Si crystallinity during first Li<sup>+</sup> insertion, prevented the structural change of Si-based materials from being fully understood. Naturally, the way in which Si-based materials degrade during cycling could not be figured out. So, there was a reasonable need to elucidate the nanoscale phase transition that Si has to undergo during Li<sup>+</sup> insertion or extraction.<sup>8,9</sup> Our previous work not only clarified some of phase transitions in the lithiated silicon but also showed that the clarified phase transition (Li<sub>x</sub>Si-to-Li<sub>15</sub>Si<sub>4</sub> transition) results in an enormous volume expansion, followed by the severe cyclic degradation of Si-based materials.<sup>10</sup> Nevertheless, there was an opaque point about the structure of lithiated silicon (Li<sub>x</sub>Si), which is formed by the initial lithiation into Si. Actually, most of the previous work insisted that Si should change into amorphous lithium silicide in the initial stage of Li<sup>+</sup> insertion. However, considering that the amorphous state has more open structure than the crystalline one, huge volume expansion during Li<sub>x</sub>Si-to-Li<sub>15</sub>Si<sub>4</sub> transition let us wonder if Li<sub>x</sub>Si is completely amorphous or not. In addition, crystalline lithium

\*To whom correspondence should be addressed. Tel: +82-41-521-9378. Fax: +82-41-568-5778. E-mail: dake@kaist.ac.kr (present) and dake@kaist.ac.kr or dake1234@kongju.ac.kr (future).

(1) Bruce, P. G.; Scrosati, B.; Tarascon, J. M. *Angew. Chem., Int. Ed.* **2008**, *47*, 2930.  
(2) Grigoriant, I.; Sominski, L.; Li, H.; Ifargan, I.; Aurbach, D.; Gedanken, A. *Chem. Comm.* **2005**, *7*, 921.  
(3) Ng, S. H.; Wang, J.; Wexler, D.; Konstantinov, K.; Guo, Z. P.; Liu, H. K. *Angew. Chem., Int. Ed.* **2006**, *45*, 6896.  
(4) Kim, H.; Cho, J. *Nano Lett.* **2008**, *8*, 3688.  
(5) Winter, M.; Besenhard, J. O. *Electrochim. Acta* **1999**, *45*, 31.  
(6) Chan, C. K.; Peng, H.; Liu, G.; McIlwrath, K.; Zhang, X. F.; Huggins, R. A.; Cui, Y. *Nat. Nanotechnol.* **2008**, *3*, 31.

(7) Hatchard, T. D.; Topple, J. M.; Fleischauser, M. D.; Dahn, J. R. *Electrochem. Solid-State Lett.* **2003**, *6*, A129.  
(8) Obrovac, M. N.; Christensen, L. *Electrochem. Solid-State Lett.* **2004**, *7*, A93.  
(9) Lacroix-Orio, L.; Tillard, M.; Zitoun, D.; Belin, C. *Chem. Mater.* **2008**, *20*, 1212.  
(10) Kang, Y. M.; Lee, S. M.; Kim, S. J.; Jeong, G. J.; Sung, M. S.; Choi, W. U.; Kim, S. S. *Electrochem. Commun.* **2007**, *9*, 959.

silicides such as  $\text{Li}_{12}\text{Si}_7$ ,  $\text{Li}_7\text{Si}_3$ ,  $\text{Li}_{13}\text{Si}_4$ ,  $\text{Li}_{22}\text{Si}_5$ , have much lower formation Gibbs free energy than amorphous Lithium silicide.<sup>11</sup> ( $\Delta G(\text{Li}_{12}\text{Si}_7, \text{Li}_7\text{Si}_3, \text{Li}_{13}\text{Si}_4, \text{Li}_{22}\text{Si}_5) = -199.5, -109.9, -183.9, -273.3$  kcal/mol;  $\Delta G(\text{a-LiSi}_{0.47}) = -4.15$  kcal/mol)

Herein, TEM (transmission electron microscopy)-EELS (electron energy loss spectroscopy) analysis was conducted to figure out the nanoscale phase transitions of Si-based materials during the electrochemical reaction. EELS is a powerful technique to analyze the unoccupied states above the Fermi level with sub nanometer spatial resolution. The theoretical simulation of the core-hole effect can be achieved by using an explicit core-hole, for instance by generating an atomic pseudopotential with one core electron missing, or by replacing the regarded atom in the supercell by one of the next heavier chemical element of the periodic table, like a substitutional impurity atom in the supercell.<sup>12</sup> It has been well-established that atom and orbital resolved p-DOS (partial density-of-states) in the conduction band is a reasonable approximation to the EELS spectra.<sup>13–17</sup> Hence, the nanoscale phase transitions of Si-based materials during the electrochemical reaction was investigated by comparing Si K-edge spectra from EELS with p-DOS from the theoretical calculation, which is called first-principle calculation.

## Experimental Section

**(1) Electrochemical Measurements for Si and Si-Based Materials.** To evaluate the electrochemical characteristics, electrodes were fabricated using the mixture, which was composed of 85 wt % active material (bare Si or Si based materials) and 5 wt % Super P carbon. A solution containing 10 wt % PI (Poly Imide) binder in n-methyl-2-pyrrolidinone (NMP) was added to the mixture. Cu foil was then used to coat the mixture. Even after the electrode was dried at 110 °C for 2 h in a vacuum ( $1 \times 10^{-3}$  Torr), it was not compressed to get a proper porosity. Even if we gave a little porosity to the electrode to prevent the unwanted lift-off of Si powders, the measured dilation seems to directly reflect the stress that Si powders undergo when using a stiff binder like PI. The coin-type half cells were used for the charging/discharging experiment. The assembly was carried out in an Ar-filled glovebox with less than 1 ppm each of oxygen and moisture. Li metal foil was used as the counter electrode and reference electrode, 1 M  $\text{LiPF}_6$  in ethylene carbonate and diethyl carbonate (3:7) was used as the electrolyte, and Celgard 2400 was used as the separator.

**(2) Structural Characteristics and Ab initio Calculation for Si.** The morphology and microstructure of Si during  $\text{Li}^+$  insertion was characterized by TEM analysis. To figure out the electronic density of states of Si, we adopted EELS analysis. For EELS analysis, electron transparent samples were required. This was achieved by crushing powders and then suspending them in anhydrous dimethylcarbonate (DMC). These specimens were deposited on nickel grids coated with lacey carbon film. For sample sensitive to air (cycled materials), the preparation was performed in an argon-filled drybox and transferred into the microscope using a vacuum transfer holder. The energy positions of Si K-edge for lithiated silicon during the electrochemical  $\text{Li}^+$  insertion were compared with the simulated p-DOS obtained from ab initio calculation.

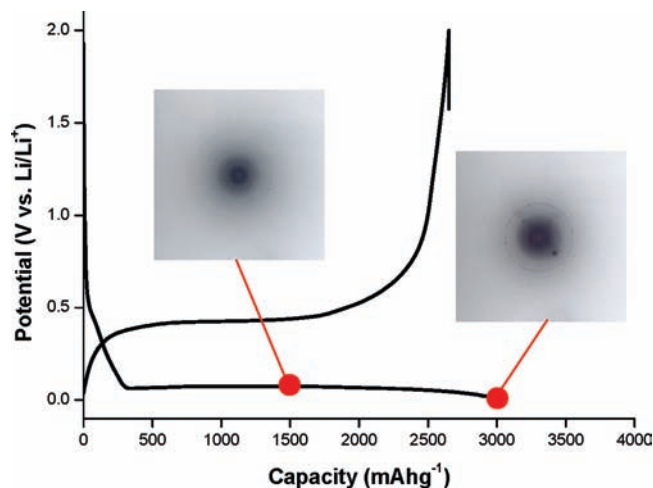


**Figure 1.**  $\text{Li}^+$ -inserted states, where TEM-EELS analyses were conducted for Si. SADP (selected area diffraction pattern) of lithium silicides obtained at the indicated points.

The CASTEP ab initio simulation package was used in this study to calculate both electronic structure and electron-energy-loss-function of bulk silicon and lithiated silicon during  $\text{Li}^+$  insertion.<sup>15</sup> The CASTEP, a plane-wave pseudopotential total energy package utilizes the DFT (density functional theory) and works within the framework of the local density approximation (LDA).<sup>16,17</sup> The electron-ion interaction is described by using a nonconserving pseudopotential. All the total energy data were available with a 340 eV energy cutoff. We used a  $6 \times 6 \times 6$  Monkhorst-Pack k-point sampling for bulk silicon and  $\text{Li}_7\text{Si}_3$ ,  $2 \times 2 \times 2$  for  $\text{Li}_{15}\text{Si}_4$ ,  $4 \times 4 \times 3$  for LiSi and  $2 \times 1 \times 6$  and for  $\text{Li}_{13}\text{Si}_4$ . The LDA method underestimates the band gap in both semiconductors and insulators. To adjust the band gap, we estimated the DOS and p-DOS with Hatree-Fock method.

**(3) Investigation on the Thickness Variation of Electrode Including Si-Based Materials.** In situ load cell systems, which are composed of gap sensor and a linear voltage displacement transducer, have been used to measure the electrode swelling during electrochemical cycling under compressive stress. The shape of designed electrode for load cell systems was a typical coin-type. With this type of load cell systems, we have investigated the thickness variation of electrode during cycling. Depending on the sort of electrode materials as well as the potential range for electrochemical reaction, our load cell systems have shown some interesting results in the thickness variation of electrode. Because the result from load cell system was completely equal to that obtained by a direct measurement using micrometer, the thickness variation from load cell system has been regarded as an absolutely reasonable result.

## Results & Discussion

Even though the previous research kept telling us that Si is sure to first transform into amorphous lithium silicides during  $\text{Li}^+$  insertion, we had several logical grounds on which we could doubt whether the initial nanostructure of lithium silicides is completely amorphous or not. Supposing that amorphous lithium silicides may tend to have lower density than crystalline lithium silicides, we could not encounter the colossal volume expansion observed during  $\text{Li}_x\text{Si}$ -to- $\text{Li}_{15}\text{Si}_4$  transition. Besides, crystalline lithium silicides are thermodynamically preferred when amorphous lithium silicides and crystalline lithium silicides are compared in terms of formation Gibbs free energy.<sup>10,11</sup> Therefore, there was an essential need to figure out the nanostructure of lithium silicides formed at the initial stage of  $\text{Li}^+$  insertion into Si.

(11) Limthongkul, P.; Jang, Y. I.; Dudney, N. J.; Chiang, Y. M. *Acta Materialia* **2003**, *51*, 1103.

(12) Elsasser, C.; Kostlmeier, S. *Ultramicroscopy* **2001**, *86*, 325.

(13) Egerton, R. F. *Electron Energy Loss Spectroscopy in the Electron-Microscope*; Plenum: New York, 1996.

(14) Brown, F. C.; Cahwiller, C.; Kunz, A. B.; Lipari, N. O. *Phys. Rev. Lett.* **1970**, *25*, 927.

(15) Payne, M. C.; Teter, M. P.; Allan, D. C.; Arias, T. A.; Joannopoulos, J. D. *Rev. Mod. Phys.* **1992**, *64*, 1045.

(16) Ceperley, D. M.; Alder, B. J. *Phys. Rev. Lett.* **1980**, *45*, 566.

(17) Perdew, J. P.; Zunger, A. *Phys. Rev. B* **1981**, *23*, 5048.

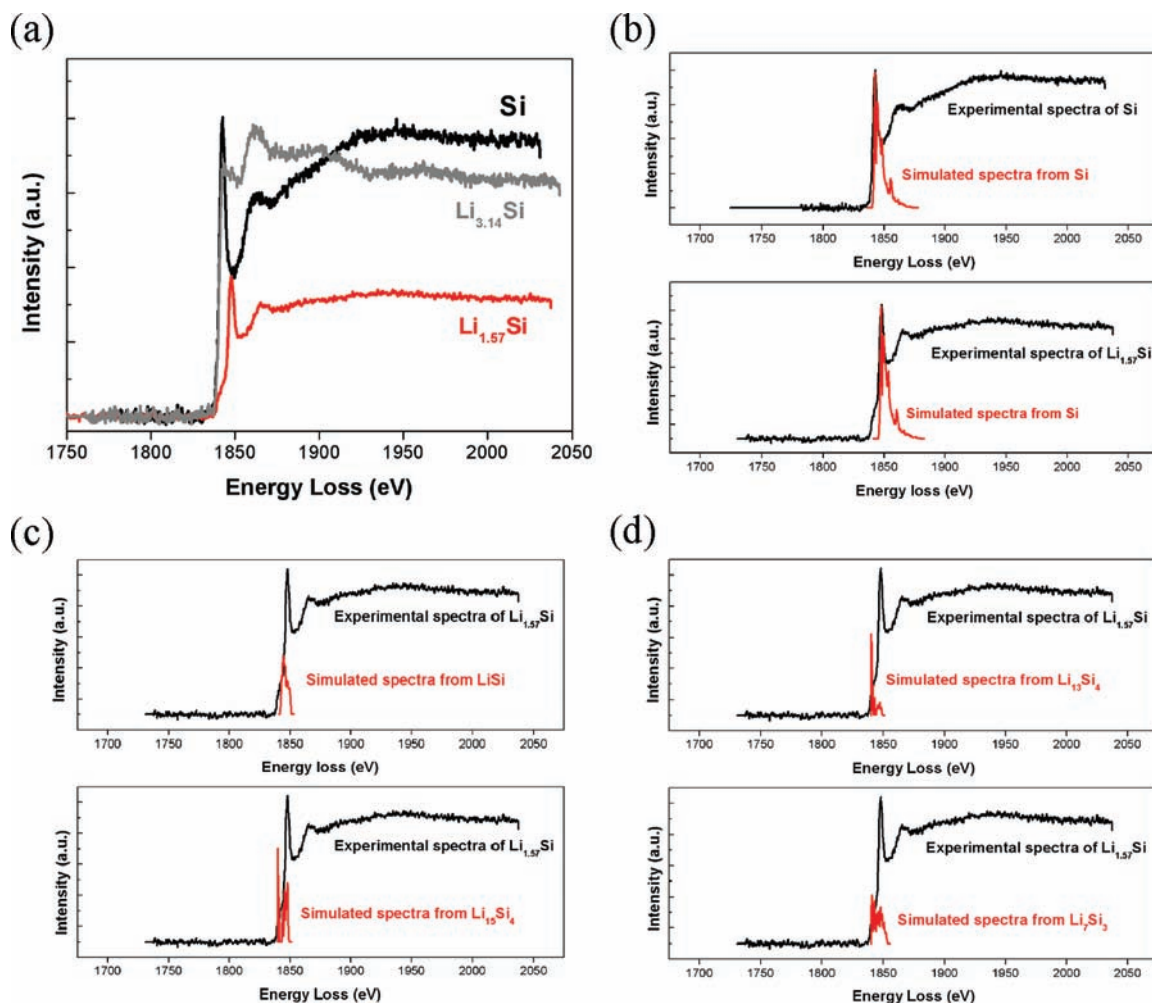


**Figure 2.** (a) Si K-edge spectra obtained from EELS analysis. The comparison between experimental and simulated Si K-edge spectra: (b) experimental, Si,  $\text{Li}_{1.57}\text{Si}$ ; simulated, Si; (c) experimental,  $\text{Li}_{1.57}\text{Si}$ ; simulated,  $\text{LiSi}$ ,  $\text{Li}_{15}\text{Si}_4$ ; (d) experimental,  $\text{Li}_{1.57}\text{Si}$ ; simulated,  $\text{Li}_{13}\text{Si}_4$ ,  $\text{Li}_7\text{Si}_3$ .

TEM observation has confirmed the nanostructural change of Si during  $\text{Li}^+$  insertion. Figure 1 indicates the states of  $\text{Li}^+$  insertion in which TEM analysis was conducted. To discriminate the nanostructure of lithium silicide formed by a small lithiaton into Si from a crystalline phase,  $\text{Li}_{15}\text{Si}_4$ , two points have been selected as shown in Figure 1. SADP (selected area diffraction pattern) at the second point of  $\text{Li}^+$  insertion displays an apparent polycrystalline pattern that results from the crystalline phase,  $\text{Li}_{15}\text{Si}_4$ . Even though the perfect hollow ring of amorphous lithium silicide has been expected from the previous research, SADP at first point (the initial stage of  $\text{Li}^+$  insertion) is mainly composed of some opaque polycrystalline patterns. This peculiar observation notified that lithium silicides at least have a crystalline ordering even before the formation of  $\text{Li}_{15}\text{Si}_4$ . However, it was extremely difficult to figure out which phase is related to this polycrystalline pattern. EELS, which enables the electronic density of states to be probed at nanometer scale is an effective analytic method to disclose the chemical state of materials.<sup>12,13</sup> When EELS was combined with p-DOS obtained from first-principle calculation, the microstructure of material has been comprehensively understood. In addition, because an ion situated on a surface has more degrees of freedom than an ion constituting a part of a three-dimensionally periodic crystal lattice, the problem of first-principle calculation of the electronic structure of a surface turns out to be far more

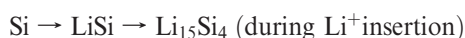
demanding computationally than the corresponding bulk problem. EELS is a completely adaptable method to elucidate not only the surface electronic structure of lithiated silicon but also its bulk electronic structure. Therefore, Si K-edge spectra of lithium silicides from EELS have been compared with their p-DOS from the theoretical calculation.<sup>18</sup> Total DOS's (density-of-states) of Si and lithium silicides such as  $\text{LiSi}$ ,  $\text{Li}_{15}\text{Si}_4$ ,  $\text{Li}_7\text{Si}_3$ , and  $\text{Li}_{13}\text{Si}_4$  have been simulated from Hartree–Fock method. (see Figure S1 in the Supporting Information; it was assumed that the Fermi energy is 0 eV.) Even if the Hartree–Fock method definitely involves the underestimation of band gap followed by an excessive calculation time, it features the accurate evaluation of exchange potential and band gap and makes it possible to completely simulate the structure of empty band.<sup>18</sup> From total DOS, it was known that  $\text{Li}_{15}\text{Si}_4$ ,  $\text{Li}_7\text{Si}_3$ , and  $\text{Li}_{13}\text{Si}_4$  are conducting materials without a band gap, whereas  $\text{LiSi}$  is a semiconducting material with a constant band gap. Figure 2a is Si K-edge spectra obtained from EELS analysis. The comparison between Si K-edge spectra of Si and  $\text{Li}_{1.57}\text{Si}$  (the initial stage of  $\text{Li}^+$  insertion) clearly shows that there is some difference in the shape of spectra. When we focus on Si K-edge spectra of  $\text{Li}_{1.57}\text{Si}$ , a small hump in front of the main peak around 1845 eV

(18) Dudarev, S. L.; Botton, G. A.; Savrasov, S. Y.; Szotek, Z.; Temmerman, W. M.; Sutton, A. P. *Phys. Status Solidi A* **1998**, *166*, 429.

informs that another phase is evolved except for Si. This observation is well-matched with an abrupt emergence of novel polycrystalline phase in SADP (Figure 1) of  $\text{Li}_{1.57}\text{Si}$ . Also in the Si thin film, it has been disclosed by Raman spectroscopy that only a small amount of  $\text{Li}^+$  insertion initiates the phase transition from amorphous Si to polycrystalline lithium silicide.<sup>19</sup>

As shown in Figure 2b, both the experimental edge spectra of Si and the simulated one have similar peaks located around 1840 eV. Even if the simulated one is slightly down-shifted to low energy-loss region compared to the experimental one, the former is tolerably in accordance with the latter in the shape and trend of peak. Hence, it was known that our first-principle calculation based on density functional theory completely establishes a reliable simulation well-fitted with the experimental results. In panels c and d in Figure 2, the simulated Si K-edge spectra for various crystalline lithium silicides ( $\text{LiSi}$ ,  $\text{Li}_{15}\text{Si}_4$ ,  $\text{Li}_7\text{Si}_3$ , and  $\text{Li}_{13}\text{Si}_4$ ) also display the down shift in energy loss compared to the experimental one for  $\text{Li}_{1.57}\text{Si}$ . When focusing on the shape and trend of peaks, it can be easily observed that the simulation for  $\text{LiSi}$  generates the most similar result to the experimental Si K-edge spectra of  $\text{Li}_{1.57}\text{Si}$ . On the other hand, the simulated peaks for  $\text{Li}_7\text{Si}_3$  and  $\text{Li}_{13}\text{Si}_4$  show a clear difference with the experimental one because they feature a typical DOS of conductor.

In Figure 3a, the experimental spectra of  $\text{Li}_{1.57}\text{Si}$  were compared with the simulated ones for  $\text{LiSi}$  and Si. Herein, the simulated ones seem to be deconvoluted from the experimental one. Therefore, we could know that the crystalline ordering of Si coexists with that of  $\text{LiSi}$  when 1.57 mol of  $\text{Li}^+$  react with Si (before the formation of  $\text{Li}_{15}\text{Si}_4$ ). Figure 3b consists of the experimental edge spectra of  $\text{Li}_{3.14}\text{Si}$  after the complete lithiation and the simulated one for  $\text{Li}_{15}\text{Si}_4$ . The experimental peaks located in 1844 and 1848 eV correspond to the simulated ones in 1842 and 1850 eV, respectively. The peak located around 1860 eV in the experimental spectra may be related to the remaining Si. So, it can be concluded that the final phase during  $\text{Li}^+$  insertion is attributed to  $\text{Li}_{15}\text{Si}_4$ . By correlating the experimental observation with the theoretical calculation, it was completely figured out which phase transition Si should undergo during the electrochemical  $\text{Li}^+$  insertion. The elucidated process can be suggested as follows



The unit-cell structures of  $\text{LiSi}$  and  $\text{Li}_{15}\text{Si}_4$ , which have been obtained from first-principle calculation, are presented in the Figure 3 inset. The space group symmetry of  $\text{LiSi}$  is  $4/m$ , whereas that of  $\text{Li}_{15}\text{Si}_4$  is  $m\bar{3}m$ . The volume of unit-cell in  $\text{LiSi}$  and  $\text{Li}_{15}\text{Si}_4$  is 502 and 1211  $\text{\AA}^3$ , respectively. When the number of atoms constituting the unit cell is considered, the volume per atom is 31  $\text{\AA}^3$  for  $\text{LiSi}$  and 76  $\text{\AA}^3$  for  $\text{Li}_{15}\text{Si}_4$ . The comparison between  $\text{LiSi}$  and  $\text{Li}_{15}\text{Si}_4$  in the volume per atom indicates that the phase transition from  $\text{LiSi}$  to  $\text{Li}_{15}\text{Si}_4$  has to involve an enormous volume expansion around 230%. Because the volume per atom of Si is 20  $\text{\AA}^3$  (the volume of the unit cell is 160  $\text{\AA}^3$ ), the volume expansion from Si to  $\text{Li}_{15}\text{Si}_4$  gets to about 380%, which is the theoretically expected value.<sup>8,10</sup> This structural explanation for volume

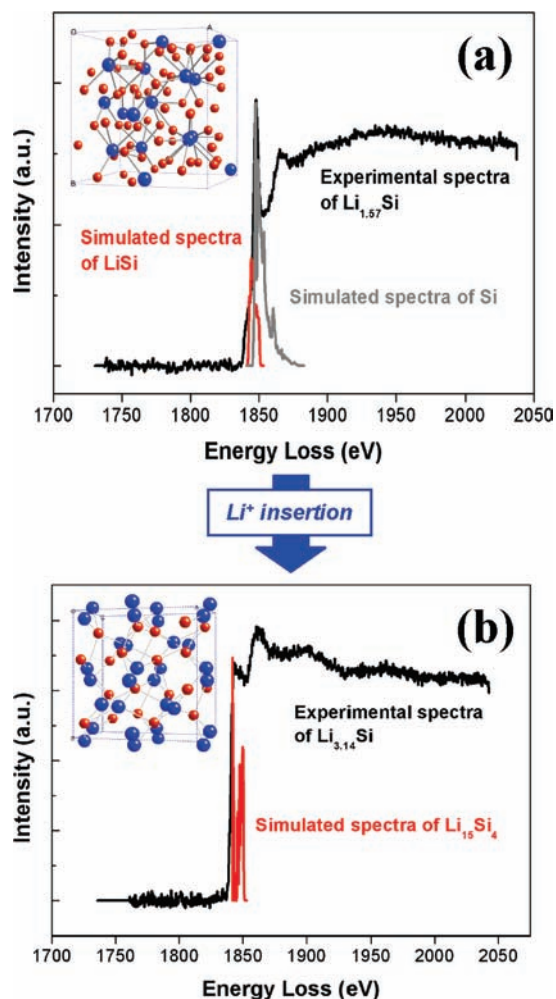


**Figure 3.** Comparison between experimental and simulated Si K-edge spectra; (a) experimental,  $\text{Li}_{1.57}\text{Si}$ ; simulated,  $\text{LiSi}$ , Si; (b) experimental,  $\text{Li}_{3.14}\text{Si}$ ; simulated,  $\text{Li}_{15}\text{Si}_4$ . The inset figures display the unit-cell structures of  $\text{LiSi}$  (space group:  $4/m$ ) and  $\text{Li}_{15}\text{Si}_4$  (space group  $m\bar{3}m$ ). The orange-colored spheres and blue-colored spheres correspond to Si atoms and Li atoms, respectively.

expansion is in great accordance with the volume expansion observed in our previous result that the volume expansion from  $\text{LiSi}$  to  $\text{Li}_{15}\text{Si}_4$  is comparable to that from Si to  $\text{LiSi}$ . The deliberation on the unit-cell structure seems to make the evolution of  $\text{LiSi}$  extremely plausible.

In situ load cell system has been used to measure the volume change of electrode including Si-based materials during electrochemical cycling. In Figure 4a, the thickness variation of the electrode is displayed to express the volume change of sample material as a numerical value. As shown here, the more  $\text{Li}^+$  inserts, the larger the volume expansion of its electrode is getting. Supposing that Si undergoes the phase transition from  $\text{LiSi}$  to  $\text{Li}_{15}\text{Si}_4$ , the expansion and contraction of volume gets irreversible even after first cycle. (route (i)) Meanwhile, when Si changes into  $\text{LiSi}$  and returns back to the original phase without the formation of  $\text{Li}_{15}\text{Si}_4$ , the electrode including Si repeats a reversible expansion and contraction (route (ii)). As shown in Figure 4b, the irreversibility of volume change is in accordance with that of capacity. The irreversibility of volume change, followed by that of capacity, can be clearly understandable considering the disparity between  $\text{LiSi}$  and  $\text{Li}_{15}\text{Si}_4$  in the volume per atom, which

(19) Ryu, Y. G.; Jung, I. S.; Lee, S. S.; Doo, S. G. *The International Society of Electrochemistry Annual Meeting Proceedings*; Edinburgh, U.K., Aug 27–Sept 1, 2006; International Society of Electrochemistry: Lausanne, Switzerland, 2006; p S1-P-56.

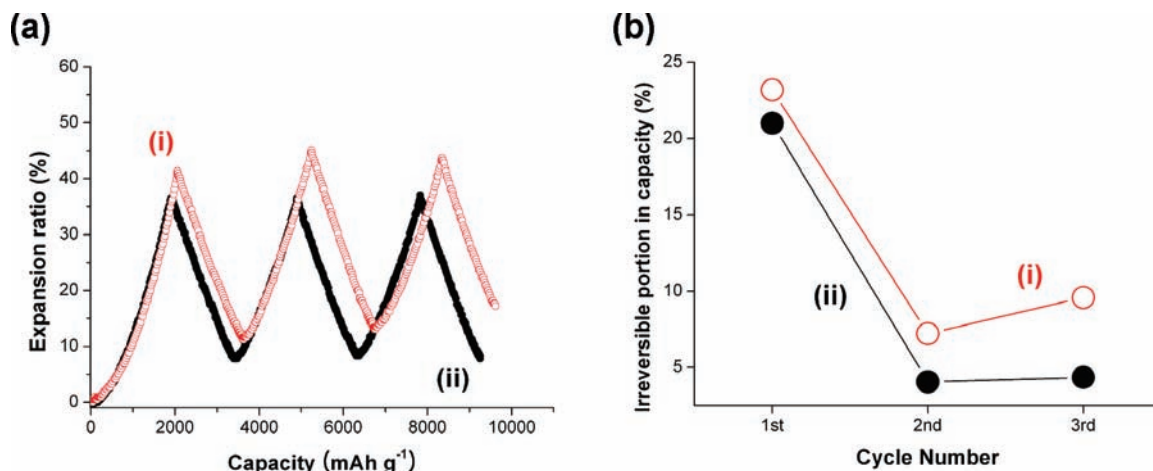


**Figure 4.** (a) Volume variation of Si-based material (oxide-coated Si) according to the phase transition route: (i)  $\text{Si} \rightleftharpoons \text{LiSi} \rightleftharpoons \text{Li}_{15}\text{Si}_4$ , (ii)  $\text{Si} \rightleftharpoons \text{LiSi}$ . (b) The irreversible capacity of Si according to the above-mentioned two phase transition routes.

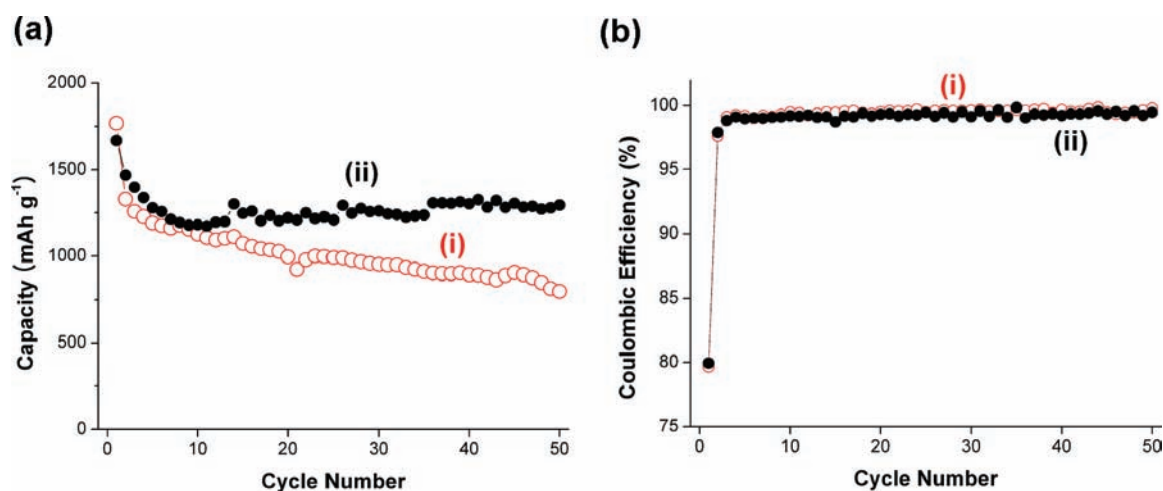


**Figure 5.** Anodic performance of Si-based materials according to the phase transition route: (i)  $\text{Si} \rightleftharpoons \text{LiSi} \rightleftharpoons \text{Li}_{15}\text{Si}_4$ , (ii)  $\text{Si} \rightleftharpoons \text{LiSi}$ . (a) Cyclic performance of Si-based materials at 0.5C and (b) the Coulombic efficiency of Si based materials up to 50th cycle.

was discussed above. Figure 5 shows the cyclic properties of Si-based material with two different phase transition routes. Also as expected in the above discussion, it can be observed that when Si continuously gets through the phase transition from LiSi to Li<sub>15</sub>Si<sub>4</sub> and the reverse transition, Si-based materials exhibit much more drastic cyclic degradation than when the phase transition from LiSi to Li<sub>15</sub>Si<sub>4</sub> is excluded. On the basis of this electrochemical comparison, the phase transition of electrode materials during cycling may be the most significant factor to determine their electrochemical performance. In addition, the correlation between *ab initio* calculation and microstructural analysis is a quite reasonable way to clarify the charge–discharge mechanism of electrode materials.

## Conclusion

In summary, TEM-EELS analysis was conducted to clarify the microstructure of lithium silicides formed at the initial stage of Li<sup>+</sup> insertion into Si. Because SADP from TEM and Si K-edge spectra from EELS featured not amorphous state but polycrystalline state, Si K-edge spectra from EELS was correlated with p-DOS from first-principle calculation to expect the phase transitions of Si-based materials during the electrochemical reaction. As a result, it was noticed that the

crystalline ordering of Si coexists with that of LiSi before the formation of Li<sub>15</sub>Si<sub>4</sub>. With this clarified phase transition, the volume expansion and charge–discharge behaviors of Si-based materials could be more apparently understood. Finally, it is expected that this work may pave a novel way to elucidate the nanoscale phase transitions, which have never been made clear.

**Acknowledgment.** The authors thank Dr. Ju-Cheol Park at Samsung Advanced Institute of Technology, Dr. Wan-Uk Choi and Dr. Young-Ugk Kim at Samsung SDI, and Dr. Young-Min Kim at Korea Basic Science Institute (Republic of Korea) for their collaboration. This work was supported by the Korea Research Foundation Grant funded by the Korean Government (MOEHRD, Basic Research Promotion Fund) (KRF-2008-331-D00247) and Basic Science Research Program through the National Research Foundation of Korea (NRF) funded by the Ministry of Education, Science and Technology (2009-0072972).

**Supporting Information Available:** Additional figure (PDF). This material is available free of charge via the Internet at <http://pubs.acs.org>.